OPERATIONAL AVALANCHE ACTIVITY MONITORING USING RADAR SATELLITES: FROM NORWAY TO WORLDWIDE ASSISTANCE IN AVALANCHE FORECASTING

Markus Eckerstorfer[1,*], Eirik Malnes[1], Hannah Vickers[1], Karsten Müller[2], Rune Engeset[2], Tore Humstad[3]

[1]*Norut Northern Research Institute, Tromsø, Norway*
[2]*Norwegian Water Resources and Energy Directorate, Oslo, Norway*
[3]*Norwegian Public Roads Administration, Molde, Norway*

ABSTRACT: The seemingly simple questions of when and where avalanches have released are difficult to answer for large avalanche forecasting regions, especially during severe weather conditions. This imposes significant uncertainty to the regional avalanche forecasts. We have developed an innovative solution to this problem. We built an automatic processing chain that within roughly one hour after Sentinel-1 image acquisition downloads the radarsatellite images, runs an avalanche detection and tracking algorithm and outputs detected avalanches and information on location, timing and extent. Sentinel-1 data is freely and consistently available and independent of light and weather conditions. Therefore, operational avalanche activity monitoring became feasible and was tested in four forecasting regions in Norway. In this paper, we introduce the technical solutions behind our automatic processing chain, evaluate the avalanche detection algorithm's performance (82 % maximum correct detection rate) and show results from two forecasting regions in Northern Norway from the winters of 2016-2017 and 2017-2018. As the Sentinel-1 constellation covers the entire planet, we evaluate the feasibility of avalanche detection in any snow-covered mountain area worldwide.

Keywords: avalanche detection, operational avalanche activity monitoring, Sentinel-1, radar, Norway

1. INTRODUCTION

In conventional avalanche forecasting, avalanche occurrences are considered as class 1 stability data of low uncertainty (McClung, 2002). This implies that consistent and reliable spatio-temporal information on avalanche occurrences exist. However, the seemingly simple question of when and where avalanches have released in a given forecasting region is with conventional field monitoring not answerable.

We have developed an innovative solution to this problem by building an automatic avalanche detection algorithm that detects avalanche debris in radar satellite images provided by the Sentinel-1 constellation (Vickers et al., 2017). This detection algorithm is built into a near-real time processing chain that within roughly an hour after radar image download produces a geodatabase with detected avalanches and associated metadata on timing, location and size.

This paper presents our operational avalanche detection processing chain and evaluates its performance. Following this technical description, we briefly present the algorithm's raw data output exemplified on two winters of avalanche detections in Northern Norway. Finally we assess if operational avalanche detection using Sentinel-1 is feasible globally.

*Corresponding author address:
Markus Eckerstorfer, Norut Northern Research Institute, P.O. Box 6434, Tromsø Science Park, 9294 Tromsø, Norway;
email: markus.eckerstorfer@norut.no

2. DATA AND METHODS

2.1. Automatic avalanche detection processing chain

We have developed an automatic avalanche detection processing chain that (1) downloads Sentinel-1 images, (2) pre-processes them, (3) runs them through an avalanche detection algorithm and a (4) tracking algorithm and (5) outputs detected avalanches and meta-information on avalanche extent and location (Figure 1). Avalanches are detectable due to their high surface roughness compared to undisturbed snow surrounding them (Eckerstorfer and Malnes, 2015) (Figure 1).

(1) Downloading of Sentinel-1 images is done via the Copernicus Open Access Hub (https://scihub.copernicus.eu/).

(2) Pre-processing involves geocoding and terrain correction of single backscatter images and the construction of change detection image pairs showing changes in backscatter within a 6-days period (Figure 1b). It also involves the construction of masks that delimit areas where avalanche debris can occur, thus areas affected by radar shadow and layover effects, water bodies, dense forests and too steep slopes are masked out.

(3) The avalanche detection algorithm applies dynamic thresholding, filtering and segmentation to

the change detection images and outputs a binary geotiff-file with avalanche and non-avalanche areas, with a minimum avalanche size of 10 pixel. A detailed description of the algorithm is given in Vickers et al (2017).

(4) The tracking algorithm then transforms the avalanches into vectors and stores meta information on avalanche size and location. It also associates repeated detection of the same avalanche within a 6-days repeat cycle and aggregates them over time, updating the meta information (Figure 1c, d). Due to variable observation geometries the avalanche outline may be slightly changed from the first to the last observation.

(5) We delivered the automatic avalanche detections to the Norwegian Avalanche Warning Service on a daily basis during the winter 2017-2018 in four forecasting areas in Norway.

3. RESULTS

3.1. Operational avalanche detection in Norway

We have provided the Norwegian Avalanche Warning Service with avalanche detections in an operational manner for the last two winters (2016-2017 and 2017-2018) in four different forecasting regions. The data was made available via a FTP-server. In the winter 2018-2019, the processing chain will be run by the Norwegian Avalanche Warning Service, incorporating the avalanche detections in their technical data information system that is used by the forecasters in their decision making process.

Here we present raw results from two forecasting areas (Troms and Lyngen) in Northern Norway. We re-ran both winters with the newest versions of the detection and tracking algorithms. The study area encompassing both forecasting regions is roughly 120 x 90 km large, located at around 70 deg N.

3.2. Sentinel-1 coverage

Due to the high latitude of the study area, 477 and 486 Sentinel-1 images were available in the winters 2016-2017 and 2017-2018 respectively, resulting in two images per day. These images covered the area partly or completely. In Figure 2 we show the coverage i.e. the number of satellite acquisitions per pixel in the avalanche runout areas within a 6-days repeat cycle. There is a general inhomogeneity in coverage, however, a minimum of 4 images within 6 days is given. Steep terrain can be covered as little as 1-2 times every 6 days due to layover and radar shadow effects. The average coverage is 5.9 observations per cycle with a small fraction of pixels (0.8%) having no coverage within 6 days.

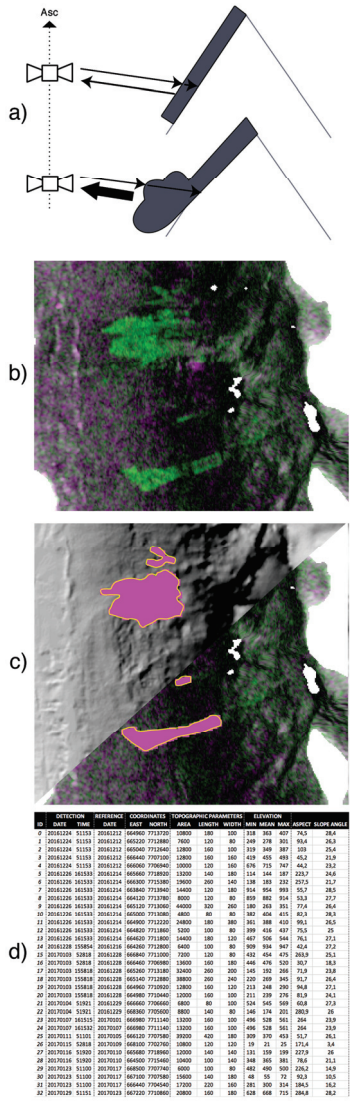

ID	DETECTION DATE	DETECTION TIME	REFERENCE DATE	COORDINATES EAST	COORDINATES NORTH	TOPOGRAPHIC PARAMETERS AREA	LENGTH	WIDTH	ELEVATION MIN	MEAN	MAX	ASPECT	SLOPE ANGLE
0	20161224	51153	20161212	664960	7713720	10800	180	100	318	363	407	74,5	28,4
1	20161224	51153	20161212	665220	7712880	7600	120	80	249	278	301	93,4	26,3
2	20161224	51153	20161212	665040	7712640	12800	160	100	319	349	387	103	25,4
3	20161224	51153	20161212	666440	7707100	12800	160	160	419	455	493	45,2	21,9
4	20161224	51153	20161212	666060	7706840	10000	120	160	676	715	747	44,2	23,2
5	20161226	161533	20161214	665660	7718920	13200	140	180	114	144	187	223,7	24,6
6	20161226	161533	20161214	666300	7715380	19600	260	140	138	183	232	257,5	21,7
7	20161226	161533	20161214	663840	7713940	14400	120	180	914	954	993	55,7	28,5
8	20161226	161533	20161214	664120	7713780	8000	120	80	859	882	914	53,3	27,7
9	20161226	161533	20161214	665120	7713060	44000	320	260	180	263	351	77,4	26,4
10	20161226	161533	20161214	665000	7713080	4800	80	80	382	404	415	82,3	28,3
11	20161226	161533	20161214	664900	7712220	24800	180	180	361	388	410	99,1	26,5
12	20161226	161533	20161214	664820	7711860	5200	100	80	399	416	437	75,5	25
13	20161226	161533	20161214	664620	7713800	14400	180	120	467	506	544	76,1	27,1
14	20161228	155854	20161216	664260	7712800	6400	100	80	909	934	947	42,4	27,2
15	20170103	52818	20161228	666840	7711000	7200	120	80	432	454	475	263,9	25,1
16	20170103	52818	20161228	666460	7709880	13600	160	180	446	476	520	30,7	18,3
17	20170103	155818	20161228	665260	7713180	32400	260	200	145	192	266	71,9	23,8
18	20170103	155818	20161228	665140	7712880	38800	260	240	220	269	345	91,7	26,4
19	20170103	155818	20161228	664960	7710920	12800	160	120	213	248	290	94,8	27,1
20	20170103	155818	20161228	664980	7710440	12000	160	100	211	239	276	81,9	24,1
21	20170104	51921	20161229	666660	7706660	6800	80	100	524	545	569	60,8	27,3
22	20170104	51921	20161229	668360	7705600	8800	140	80	146	174	201	280,9	26
23	20170107	161525	20170101	666980	7711140	13200	160	100	496	528	561	264	23,9
24	20170107	161532	20170107	666980	7711140	13200	160	100	496	528	561	264	23,9
25	20170111	51101	20170105	666120	7707580	39200	420	180	309	370	453	51,7	26,1
26	20170115	52818	20170109	668100	7702760	10800	120	120	19	21	25	171,4	3,4
27	20170116	51920	20170110	665880	7718960	12000	140	140	131	159	199	227,9	26
28	20170116	51920	20170110	664500	7715460	10400	100	140	348	365	381	78,6	21,1
29	20170123	51100	20170117	668500	7707740	6000	100	80	482	490	500	226,2	14,9
30	20170123	51100	20170117	667100	7707580	15600	140	180	48	55	72	92,3	10,5
31	20170123	51100	20170117	666440	7704540	17200	220	160	281	300	314	184,5	16,2
32	20170129	51151	20170123	667220	7710860	20800	160	180	628	668	715	284,8	28,2

Figure 1: The principle of avalanche detection with radar sensors and a graphic representation of the steps involved in the automatic processing chain from raster-based avalanche detection to vectorization and storage in a geodatabase.

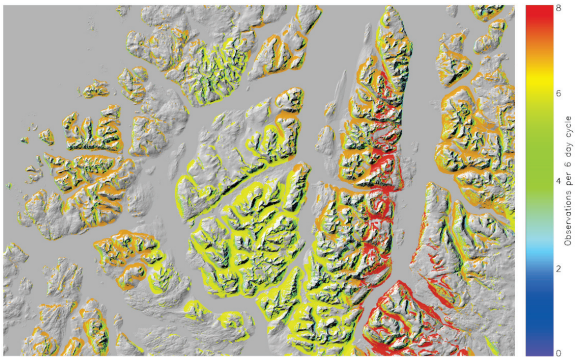

Figure 2: Sentinel-1 image coverage in avalanche runout areas per 6 day repeat cycle.

3.3. Algorithm performance

We validated the performance of the detection and tracking algorithm against manual interpretation in

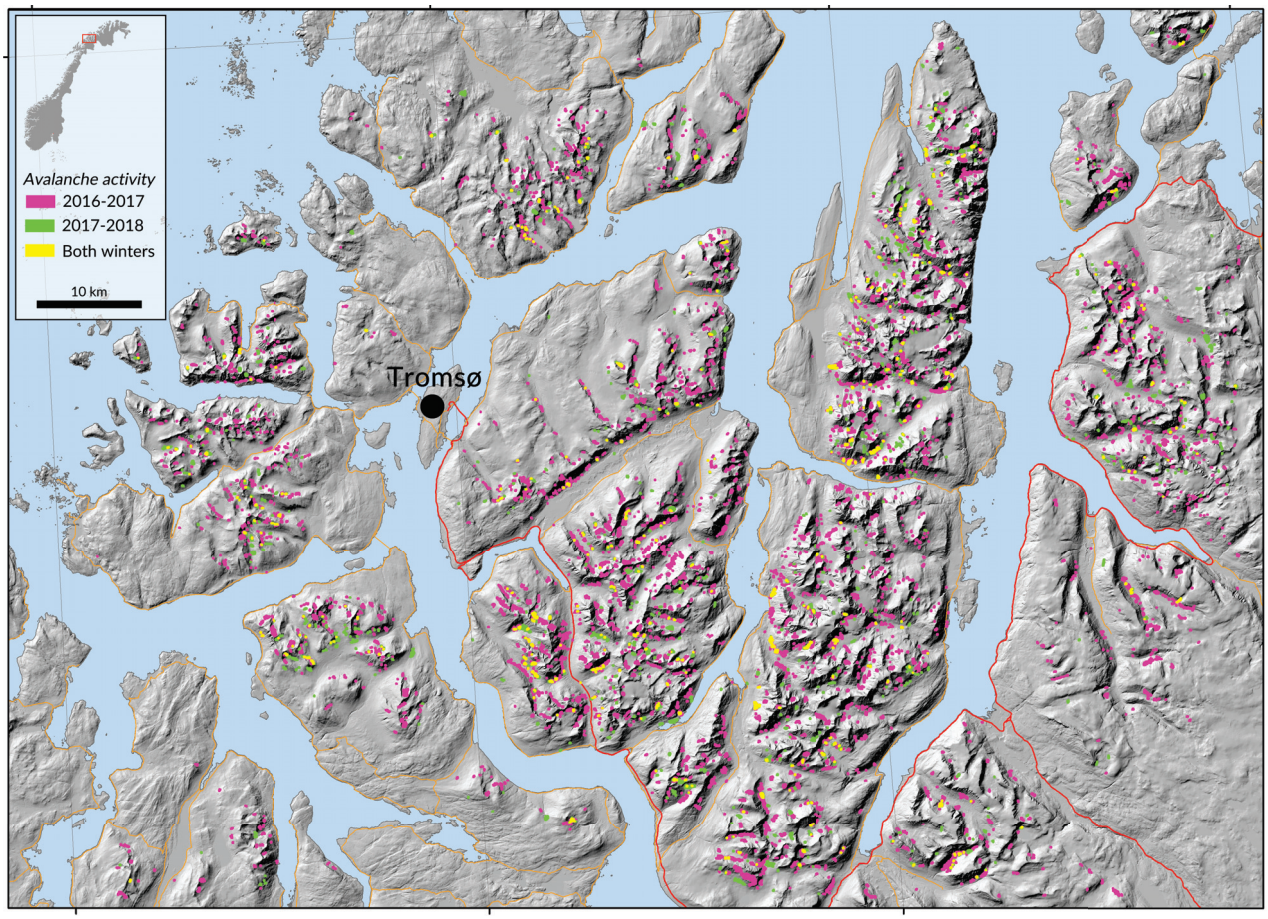

Figure 3: Topographic map of the study area around the city of Tromsø, Northern Norway with detected avalanche activity colored according to winter.

six images. The probability of detection (POD) ranged between 82.0% and 55.7% with corresponding false alarm rates (FAR) of 26.4% and 13.8%. Heidke Skill Scores (HSS) ranged between 0.599 and 0.425 respectively. The variation in detection performance stems largely from the algorithm's dependency on the snow conditions in the change detection images. If snow went from dry to wet, which resulted in a net decrease in backscatter in the change detection image, avalanches were detectable with POD's ranging in the 80% range. The reason is the large backscatter difference between avalanches and surrounding undisturbed wet snow, as avalanches exhibit relative high backscatter due to their rough surface. Vice versa, a net decrease in backscatter as a consequence of wet snow turning dry, resulted in a small relative backscatter difference between avalanches and surrounding snow. The algorithm then tended to overdetect and falsely delineate large slopes as avalanches.

3.4. Automatically detected avalanche activity

With these shortcomings in mind, we present a map with detected avalanche activity from two winters (2016-2017 and 2017-2018) without any post-processing to eliminate known false alarms (Figure 3). A qualitative examination of the meteorological records reveal quite different meteorological conditions in both winters. 2016-2017 was characterized by highly fluctuating air temperatures accompanied with either heavy rain or snow from frequent low-pressure activity. 2017-2018 on the other hand was characterized by a prolonged dry and cold spell from mid January to end of March. This resulted in nearly 80% more avalanches detected in winter 2016-2017 than in winter 2018-2019. Due to the higher avalanche activity in 2016-2017, the spatial occurrence of avalanche activity was larger in extent, affecting more slopes (Figure 3). A quantitative comparison of both winters, however, yields no differing spatial trend in avalanche activity between winters. In fact, nearly 70% of all avalanches in 2018-2019 overlapped with detections from 2016-2017, indicating annually avalanche prone locations (yellow markers in Figure 3). Note that a large portion of avalanche activity occurred along the exposed road network.

4. DISCUSSION AND CONCLUSION

4.1. The Sentinel-1 radar-satellite constellation

The Sentinel-1 constellation (S1A S1B) flies in a sun-synchronous near polar orbit around the globe. The satellites fly towards and from the North Pole in an ascending and descending orbit respectively. As a result, all global land masses are covered within 6 days using unique repetitive satellite paths. Using multiple satellite paths and geometries that overlap results in revisit frequencies of roughly 3 days in equatorial regions and 1 day at high latitudes.

Using radar satellite data for avalanche detection is advantageous in a number of ways. Active radar sensors illuminate Earth's surface using microwave radiation and are thus independent of weather and light conditions. The Sentinel-1 constellation delivers free radar data in a consistent manner, enabling near-real time monitoring of medium sized avalanches almost anywhere on Earth (Figure 4).

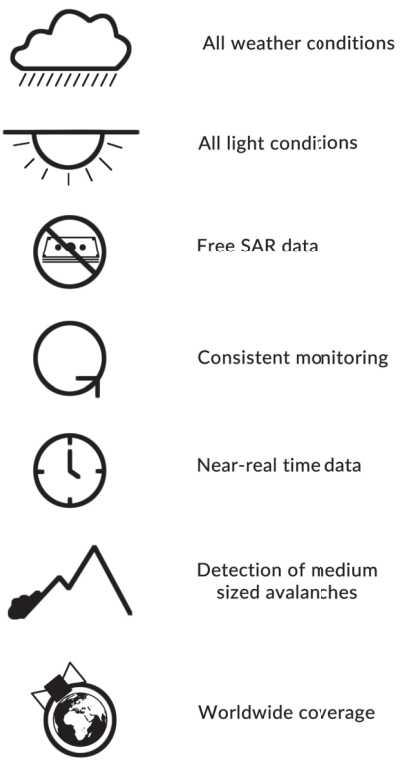

Figure 4: Key characteristics of Sentinel-1 avalanche detection.

4.2. Worldwide avalanche detection using Sentinel-1

The Sentinel-1 constellation covers all snow-covered mountain regions worldwide with the exception of the Transantarctic Mountains (Figure 5). For avalanche activity monitoring, the availability of ascending and descending orbit data is important. Only then, all slope aspects can be monitored due to the side-looking geometry of the radar sensors. All avalanche warning services in Europe can expect Sentinel-1 data with a maximum revisit frequency of 6 days, with Iceland suffering from only single orbit data. The North American avalanche forecasting regions are all covered by ascending and descending orbits with a revisit frequency of 12 days (Eckerstorfer et al., 2018).

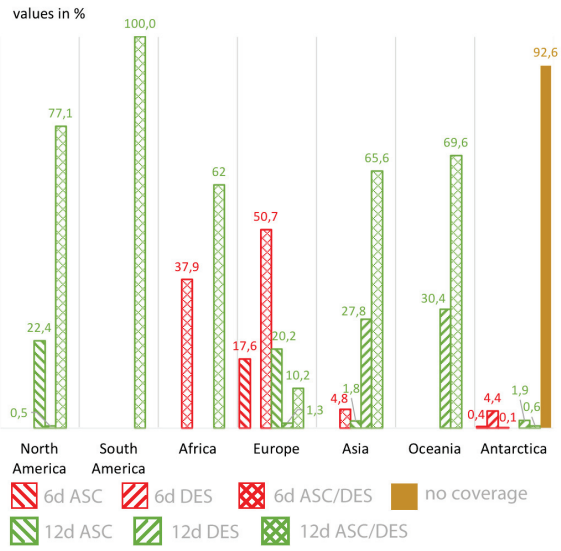

Figure 5: Relative amount of mountain regions divided by continent covered by Sentinel-1 data. Coverage frequency of multiple orbits is not considered here.

4.3. Limitations of remote sensing and road ahead

Remote sensing has its limitations. An accurate assessment of the probability of detection compared to real-world avalanche activity suffers from the comparison of datasets of very different size. We are therefore unsure how many avalanches we are not detecting. A comparison with field observations of 45 avalanches (wet and dry, D1.5-D4) in Northern Norway reveals a POD of 75%. The improvement of our understanding of which type of avalanche is detectable under which conditions is critical in improving automatic avalanche detection. We are currently collecting a dataset on surface roughness and snow parameters from different avalanche types that can be incorporated in microwave emission models of snow. We are furthermore experimenting with the use of machine learning techniques in automatically detecting avalanches in radar images in order to confidently boost the POD (see companion paper in these proceedings by Kummervold et al.).

ACKNOWLEDGEMENT

This work was financed by the Satskred 2.0 project (NIT.18.17.5), which is funded by the Norwegian

Space Centre, the Norwegian Water Resources and Energy Directorate and the Norwegian Public Road Authorities. This work is also financed by the AVAMAP project (ESA Science for Society, contract no. 4000123742/18/I-SBo) funded by the European Space Agency.

REFERENCES

Eckerstorfer, M., Malnes, E.,Vickers, H. Worldwide avalanche detection using Sentinel-1. *Service prospectus. Norut report 14/2018. ISBN: 987-82-7492-412-3* https://sites.google.com/norut.no/avamap/publications

Eckerstorfer, M., Malnes, E. Manual detection of snow avalanche debris using high-resolution Radarsat-2 SAR images. *Cold Reg. Sci. Technol. 120, 205–218.* https://doi.org/10.1016/j.coldregions.2015.08.016

McClung, D.M. The elements of applied avalanche forecasting, Part II: The physical issues and the rules of applied avalanche forecasting. *Nat. Hazards 26, 131–146.*

Vickers, H., Eckerstorfer, M., Malnes, E., Doulgeris, A. Synthetic Aperture Radar (SAR) Monitoring of Avalanche Activity: An Automated Detection Scheme in: Sharma, P., Bianchi, F.M., (Eds.) Image Analysis: 20th Scandinavian Conference, SCIA 2017, Tromsø, Norway. *Proceedings, Part II. Springer International Publishing, Cham., 136-146* https://doi.org/10.1007/978-3-319-59129-2-12